Proceedings Paper:
Sahin, A., Rey, P. and Panoutsos, G. (2022) Self-tuning multi-model statistical process control for process monitoring in additive manufacturing. In: 2022 8th International Conference on Control, Decision and Information Technologies (CoDIT). CoDIT 2022 - 8th International Conference on Control, Decision and Information Technologies (CoDIT), 17-20 May 2022, Istanbul, Turkey. Institute of Electrical and Electronics Engineers, pp. 1049-1054. ISBN: 9781665496087. ISSN: 2576-3547. EISSN: 2576-3555.

https://doi.org/10.1109/CoDIT55151.2022.9803964

Self-tuning multi-model statistical process control for process monitoring in additive manufacturing

Atakan Sahin
Automatic Control and System Engineering
The University of Sheffield
Sheffield, United Kingdom
a.sahin@sheffield.ac.uk

Pilar Rey
AIMEN Technology Centre
Polígono Industrial de Cataboi
O Porriño, E36418, Spain
prey@aimen.es

George Panoutsos
Automatic Control and System Engineering
The University of Sheffield
Sheffield, United Kingdom
g.panoutsos@sheffield.ac.uk

***Abstract*—Additive manufacturing (AM) of metals is a complex process to monitor in-situ, as the layer-by-layer deposition and material-beam interactions present a number of challenges. However, a design-driven build of customised and nearly net-shape parts makes it favourable for the manufacture of complex geometries. For process certification of critical parts there is a need for reliable process monitoring and control. Advanced thermal imaging methods can provide information in-situ, this can be used for quality assurance. Existing state-of-the-art studies based on thermal image acquisitions have the limitation of being demonstrated on simple part designs, often symmetric thin walls or cuboid structures. Statistical Process Control (SPC) has been demonstrated in past work as effective in AM, however on simple part geometries. In this work we introduce a multi-model and self-tuning computational framework for SPC via multilinear principal component analysis (MPCA), to address AM process monitoring of geometrically complex parts. In the proposed computational method, process behaviours are expressed via extracting and grouping meltpool features, thus accounting for multiple possible meltpool behaviours corresponding to part complexity and different design features. The framework operates on an iterative fashion, where the clusters (hence captured behaviours) are updated in-situ on a per-layer basis, hence continuously tuning the monitoring algorithm. A case study in blown-powder laser melting deposition of a complex geometry is presented, which includes two manufactured parts where the correlation between the predicted outliers and measured part defects is demonstrated.**

***Index Terms*—additive manufacturing, statistical process control, process monitoring, in-situ defect detection.**

I. Introduction

Additive manufacturing (AM) is a customised part construction method that enables a digital design to be built layer by layer. Expanding technologies in recent years provided the creation of complex and free form geometries unlike the conventional manufacturing practises within the many industrial sectors (such as aerospace and biomedical). The market size is predicted to have the size of $50 billion by 2031 [1]. However, the complex and free form parts require rigorous practises for quality control in the manufacturing environment. AM challenges existing quality control practises that are mostly designed for low variability and high volume manufacturing settings.

This project has been supported by the Aerospace Technology Institute, UK funding awards AIRLIFT and DAM lead by GKN Aerospace, and the EU H2020 award INTEGRADDE (grant agreement 820776).

Advanced imaging technologies have a significant role in industry to cope with the complexity that comes from the nature of the AM [2]. Furthermore, nowadays accessible computational power make an in-situ analysis of the image acquisitions feasible in practice. In situ monitoring, feedback and control have consistently been classified as one of the most-required technologies for advancing in AM [3]. Due to the small length scales and rapid solidification in AM, conventional monitoring methods fail to capture the process sufficiently. Also, there are several problems (eg. keyhole porosity, cracking, unmelted feedstock and abnormal morphology)to monitor during the deposition. Porosity and cracks are two material discontinuities that limit the quality. Porosity can be occurred due to trapped gas or the lack of fusion between the layers from the insufficient energy density. Differences in thermal expansion coefficients or powder contamination result from crackings [4]. In this context, in-situ process monitoring for AM is still in the development stage where most of the studies implemented to improve geometrical accuracy.

Statistical process control (SPC) tools are in favour to handle big data issues such high-frequency video images for in-situ monitoring purposes [5]. Even though SPC tools have been widely used for industrial process monitoring approaches, several studies have used SPC tools to propose in-situ monitoring based on image acquisition. Spatially weighted principal component analysis (PCA) is proposed via moving window updates in the modelling through the selective laser melting process [5]. This was a follow-up study for previously proposed PCA-based approach [6]. Although model updates can create changes on the control limits, pre-defined control limits were too wide to detect any abnormality due to the lack of sensitivity from a single model. Multilinear PCA (MPCA) is used for combustion monitoring [7] and blown-powder direct laser deposition image stream monitoring [8]. The complexity of the AM is not tested in [8] due to the simple geometry of the deposition. Therefore, a single and static MPCA model performs well on the selected image frames. However the single model approach, would likely fail in dealing with multiple behaviours (eg. multiple meltpool behaviours, due to multiple design features).

In this paper, an image-based, multi-model, in-situ monitoring technique based on SPC via MPCA is proposed; the

proposed also has the capability to self-tune in-situ. In the proposed method, clustering based on the meltpool features and using those separate captured behaviours for monitoring gives flexibility on how to address the complex design of AM parts which is where other studies are limited [5] and [8]. The hypothesis here is that, multiple geometrical features would give rise to separate meltpool behaviours. Capturing these behaviours separately, and analysing them (SPC via MPCA) separately, could increase the sensitivity and resolution in terms of detecting outliers (hence defects).

II. Multi-model Monitoring for Additive Manufacturing

This section includes the proposed in-situ multi-model based monitoring methodology for the detection of outliers (hence, potentially defects) in AM. SPC and its variations have been widely used in in-situ process monitoring. One of the main drawbacks for the SPC methodologies is the single model approach which limits the effectiveness (resolution, complexity) of the method. In this study, a methodology based on creating multiple monitoring models via MPCA is proposed to address this challenge.

The proposed methodology illustrated in Fig. 1 uses thermal images from an AM deposition process. The methodology starts with the pre-processing of the meltpool images for feature clustering purposes. The class labels identify the different characteristics of the deposition. PCA is extensively used in the literature for the implementation of SPC methodologies. In this study, MPCA is adopted as a dimensionality reduction mechanism. The performance metrics Hotelling's T^2 and squared prediction errors (SPE) also called Q charts are the main indicators for performance monitoring and outlier detection. Here, Hotelling's T^2 is adopted for outlier detection, where outliers are identified based on a pre-defined upper limit for the T^2 metric.

The feedback loop illustrated in Fig. 1 allows the controller involvement in the case of outlier detection and online performance improvement through the deposition. A self-tuning mechanism that updates the models (clusters) in a sliding window fashion, for a pre-defined number of layers, is used to address the changing design features, as the part is printed layer-wise. It is worth noting that, the MPCA models require the same size of input vectors, therefore, images are cropped to get lesser noise characteristics from the background where the meltpool is kept in the cropped image. This can also be done with the centralisation of the meltpool for the same size image windows. For on-axis thermal imaging tools attached to the floating robot head, the aforementioned cropping is not required where the meltpool position is tracked by the robot printing head.

A. Calculation of the Features

The first step of the feature calculation is the segmentation of the image in three regions namely: meltpool, tail and background as illustrated in Fig. 2. Depending on the resolution of the camera, the acquired image might need to be cropped to reduce the background noise, while keeping the main interest in the meltpool and tail area.

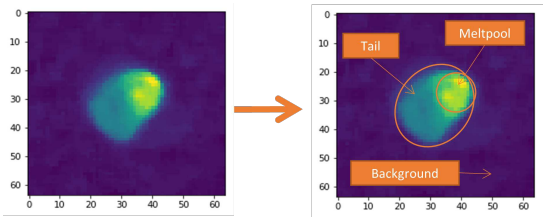

Fig. 2. Illustration of the image segmentation into three regions.

For each zone in the segmentation, an ellipse is used as an approximation, for extracting size and shape measures.

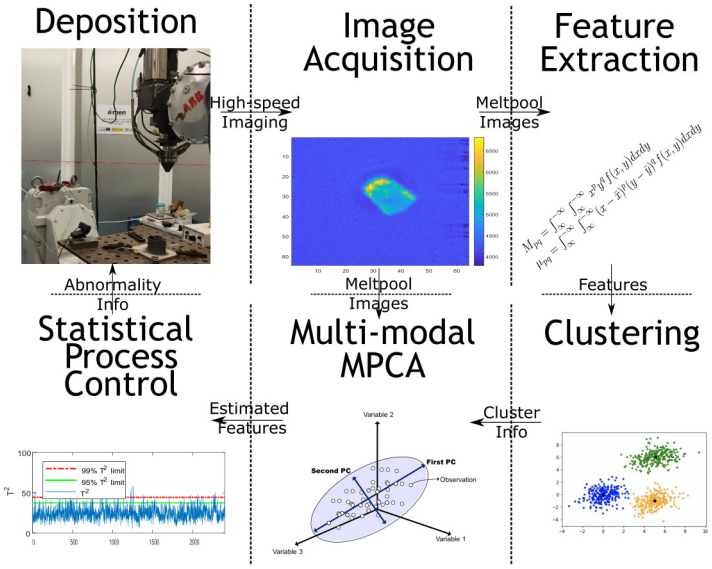

Fig. 1. Demonstration of the proposed outlier detection procedure.

Furthermore, the moments up to third order are calculated for each zone. These moments are scalar magnitudes that can be used to describe the distribution of the pixels in the image dimensions (vertical and horizontal). Due to the nature of these magnitudes, some are invariant to scale and translation, and thus, they are extremely useful in computer vision. In a total of 21 moments under 3 categories namely: raw moments, central moments where they are invariant to translation, and invariant moments where they are invariant to translation and scale. Also, thermal profiles and gradients are extracted for the two principal directions of the process, longitudinal and cross-sectional of the meltpool, and for a cross-sectional of the tail. For each image, a line is approximated following the tail direction. Using Boolean operations for a parallel of this line and its perpendicular, at the centre of the meltpool, the heat gradients are extracted. In addition to given features, area, length, width, the ratio of length to width, mean and maximum for the pre-defined areas are also extracted.

B. Feature Clustering

Well-known unsupervised clustering technique k-means clustering is used for the separation of the image characteristics. K-means aims to partition n observations in a pre-determined k number of clusters where each observation belongs to a cluster with the nearest mean. The design of the part can result in different meltpool characteristics through the deposition depending on the location and direction of the energy deposition. A set of features (n) from the different regions of the image segmentation are used for separation. Normalisation is applied to the features individually before clustering. The separation allows the multi-model approach to increase the overall sensitivity for outlier detection. Depending on the design of the deposition, some 'noise' characteristics of some regions could be meaningful deposition signatures in other regions, where the meltpool ma be showing different part-beam interactions. Cluster centres trained via the training data set transferred to the testing data set to assign clusters numbers for the new observations. This process is the same for whole the testing data until the models are re-trained again. In every new training iteration, new clusters are assigned for the same labelling where the difference between the previous cluster centres and the new cluster members are constrained.

C. Multilinear Principal Component Analysis

Multilinear PCA (MPCA) is proposed by Lu et all [9]. It is a framework for tensor object feature extraction where thermal image steams represent 3-D video sequences naturally described as tensors. MPCA performs feature extraction through the determined multilinear projections that represent captured variances from the original input. In the proposed method, a MPCA model is to be trained for each cluster defined in the clustering stage (resulting in multiple models in the system). These models are updated iteratively for a pre-defined number of deposition layers. This mechanism (self-tuning) allows for tuning the system to a 'changing' (in the z-axis) part design.

The extraction process is done iteratively by decomposing the original problem where it is $\mathbb{R}^{M\times N\times K}$ into a series of multiple projection subspace $\mathbb{R}^{P_1\times P_2\times K}$ with $P_1 < M$ and $P_2 < N$. Here, M and N are the dimensions of the video frame. MPCA is a tensor-based that can support more than 3-dimensional (3D), however, the notation is downgraded to 3D for the sake of simplicity.

A set of images can be defined as $\mathcal{X} = \mathcal{X}_{\mathbf{k}} \in \mathbb{R}^{i\times j}$ and $k = 1, ..., K$. The MPCA objective is to find a set of orthogonal transformation matrices $\widetilde{\mathbf{U}} = \{\widetilde{\mathbf{U}}^{(k)} \in \mathbb{R}^{I_k\times P_k}; \widetilde{\mathbf{U}}^{(k)^T}\widetilde{\mathbf{U}}^{(k)} = \mathbf{I}_{P_k}, P_k < I_k, k = 1, 2, 3\}$ where the projected tensor captures the most of the variation from the observations. MPCA starts with pre-processing of the observations by centring all of them as $\{\bar{\mathcal{X}} = \mathcal{X} - \bar{\mathcal{X}}\}$ where $\bar{\mathcal{X}} = \frac{1}{M}\sum_{m=1}^{M}\mathcal{X}_m$ is the sample mean. MPCA is an iterative algorithm to calculate the eigen-decomposition of

$$\mathbf{\Phi}^{(n)*} = \sum_{m=1}^{M} \widetilde{\mathbf{X}}_{m(n)} \cdot \widetilde{\mathbf{X}}_{m(n)}^{T} \tag{1}$$

and $\widetilde{\mathbf{X}}_{m(n)}$ is the n-mode of an unfolded matrix of $\mathcal{X}_{\mathbf{k}}$.

An estimated transformation matrix $\mathbf{U}^{(k)}$comprises the first and most P_n significant eigenvalues where $n = 1, 2$ of $\mathbf{\Phi}^{(n)*}$ for the meltpool image stream. Local optimisation or the iteration process of the MPCA starts with the calculation of the projection of $\widetilde{\mathcal{X}}$ onto the subspace:

$$\widetilde{\mathcal{Y}}_m = \widetilde{\mathcal{X}}_m \times_1 \widetilde{\mathbf{U}}^{(1)^T} \times_2 \widetilde{\mathbf{U}}^{(2)^T} \tag{2}$$

where $m = 1, ..., M$. Here, $\widetilde{\mathcal{Y}}_m$ captures most of the variations observed in the original tensor objects. The initialisation of the total scatter for the objective function can be done

$$\Psi_{\mathcal{Y}_0} = \sum_{m=1}^{M} \left\| \widetilde{\mathcal{Y}}_m \right\|_F^2 \tag{3}$$

where $\|\cdot\|_F$ is Frobenius norm and the mean $\bar{\widetilde{\mathcal{Y}}}$ value of $\widetilde{\mathcal{Y}}$ is all zero as $\widetilde{\mathcal{X}}$ is centred. Local optimisation continues for the number of iterations until the stopping criteria is met. For each order of the original tensor where $n = 1, 2$ for the image stream set the matrix $\widetilde{\mathbf{U}}^{(n)}$ that contains the largest P_n eigenvectors of the matrix

$$\begin{aligned}\Phi_{\mathcal{Y}_0} = \sum_{m=1}^{M} (\mathbf{X}_{m(n)} - \bar{\mathbf{X}}_{(n)}) \cdot \widetilde{\mathbf{U}}_{\Phi^{(n)}} \\ \cdot \widetilde{\mathbf{U}}_{\Phi^{(n)}}^{T} \cdot (\mathbf{X}_{m(n)} - \bar{\mathbf{X}}_{(n)})^T\end{aligned} \tag{4}$$

where

$$\begin{aligned}\widetilde{\mathbf{U}}_{\Phi^{(n)}} = \big(\widetilde{\mathbf{U}}^{(n+1)} \otimes \widetilde{\mathbf{U}}^{(n+2)} \otimes ... \otimes \widetilde{\mathbf{U}}^{(N)} \otimes \\ \widetilde{\mathbf{U}}^{(1)} \otimes \widetilde{\mathbf{U}}^{(2)} \otimes ... \otimes \widetilde{\mathbf{U}}^{(n-1)}\big)\end{aligned} \tag{5}$$

where $\otimes$ denotes the Kronecker product and $\widetilde{\mathbf{U}}^{(n)}$ is to be the solution for the optimisation subproblem of follows:

$$\widetilde{\mathbf{U}}^{(n)}, n = 1, ..., N = \underset{\widetilde{\mathbf{U}}^{(1)}, \widetilde{\mathbf{U}}^{(1)}, ..., \widetilde{\mathbf{U}}^{(N)}}{\operatorname{argmin}} \Psi_{\mathcal{Y}} \tag{6}$$

This followed by the calculation of $\{\mathcal{Y}_m, m = 1, ..., M\}$ and $\Psi_{\mathcal{Y}_k}$ until the breaking condition of the optimisation $\Psi_{\mathcal{Y}_k} -$

$\Psi_{\mathcal{Y}_{k-1}} < \eta$ is met. Here η is a pre-determined small number. After local optimisation, the feature tensor after projection can be obtained as follows for $m = 1, 2, ..., M$

$$\mathcal{Y}_m = \mathcal{X}_m \times_1 \widetilde{\mathbf{U}}^{(1)^T} \times_2 \widetilde{\mathbf{U}}^{(2)^T} \tag{7}$$

D. Statistical Process Control

Following the determination of the projected features, control chart/s such as Hoteling's T^2 multivariate cumulative sum or Q-charts can be chosen for further assessment for monitoring purposes. In process monitoring approaches, phase II approaches consider the process where online monitoring of the process is done while phase I primary interested in the assessment of the process stability. In this paper, we focus on phase II. Therefore, it is assumed that *M* images were collected from an in-control process that was worked on to design traditional control charts. First, images are used for feature extraction. Then, the features are used for clustering purposes; following the MPCA modelling for each cluster, control limits computation for the monitoring chart can be done. In this paper, T^2 charts are adopted. The Hotelling's T^2 can be used to synthesise the information from the principal components (PCs) based on pre-determined false alarm rates. For each new thermal image observation, assigned parameters for the MPCA model are applied in regards to newly assigned cluster information for the new observation. Following to low-dimensional features projection, T^2 statistic can be calculated as follows [7]:

$$T_m^2 = \frac{\left(\theta - \bar{\theta}\right)^T \mathbf{S}^{-1} \left(\theta - \bar{\theta}_I\right) N \left(M - P_1 P_2\right)}{P_1 P_2 \left(M^2 - 1\right)} \tag{8}$$

where $\bar{\theta}_I$ and $\mathbf{S}_I$ are the mean and variance-covariance matrix of the features estimated from M in-control observations by the MPCA. θ denotes the P_1P_2-dimensional vector and a positive value extracted from an observation. In applications, if the extracted features follow the multivariate normal distributions, then T^2 follow a F distribution with P_1P_2 and $M - P_1P_2$ degrees of freedom. Thereby, the control limits for T^2 can be assigned by the $(1-\alpha)100^{th}$ percentiles of the distribution. Nevertheless, the condition for the normality of the feature distribution is not met in some applications. In these conditions, an empirical distribution of T^2 can be estimated by using the training data of the in-control observations. Following the determination of α, control limits can be designed in regards to the $(1-\alpha)100^{th}$ percentiles of the distribution. The monitoring system is based on the designed control limits and T^2 statistics defined for each time frame. If the statistic exceeds the control limit, the process is evaluated as out of control and the sample evaluated as an outlier. Otherwise, the process is still in control.

P parameter for each dimension has to be determined for the calculation of the T^2 statistics. This is also the basis of the dimension reduction in the MPCA. Therefore, the objective function given in Equation 6 needs to be revised to include dimensionality reduction constraints. The Q-based method is one of the dimensionality reduction methods proposed by Lu [9] which is also the simplified one. It is based on the ratio of the total scatter in the n-mode and the remained portion of it which can be defined as follows

$$Q^{(n)} = \frac{\sum_{i_n=1}^{P_n} \lambda_{i_n}^{(n)*}}{\sum_{i_n=1}^{I_n} \lambda_{i_n}^{(n)*}} \tag{9}$$

where $\lambda_{i_n}^{(n)*}$ is the i_nth full-projection n-mode eigenvalue. Here, $\sum_{i_n=1}^{I_n} \lambda_{i_n}^{(n)*} = \Psi_{\mathcal{X}}$ for all n from Equation 4 where it is equal to total scatter for the full projection was given as $\Psi_{\mathcal{X}} = \sum_{m=1}^{M} \left\| \mathbf{Y}_{m(n)} - \bar{\mathbf{Y}}_{(n)} \right\|$ for $n = 1, ..., N$.

III. Experimental Results

The case studies for the proposed methodology is tested on thermal images acquired from laser melting depositions (LMDs). The details about the testing process and the deposition discussed in the following subsections.

A. Experimental setup

Two different depositions were used in this study to validate the accuracy of the proposed methodology. The depositions show differences in regards to laser power, scan speed, path planning and deposition material. One of the depositions can be seen in Fig. 3(a). Both parts are the same shape called c-c coupon constructed of different shapes of the walls from a single bead deposition. A blown powder-based LMD setup is used for both depositions. Image acquisition provided via high-speed coaxial medium wavelength infrared (NWIR) imaging (1 kHz) attached to the processing head with the resolution of 64×64 pixels where each pixel stands for $50 \times 50\, um$.

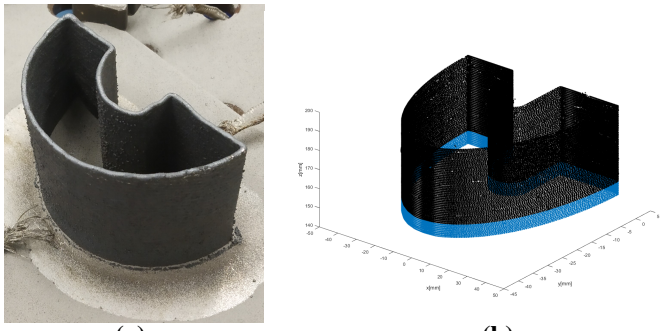

(a) **(b)**

Fig. 3. Illustration of (a) finished c-c coupon from blown-powder, laser melting deposition, (b) 3-dimensional positions of the images captured from the deposition. The first 11 layers with blue colour show the training data.

The first coupon is used path planning that requires the alternation of the direction between the layers but starts in all layers at the same point. The same alternation applied for the second coupon but the starting points changed in every layer. The laser power is set to $650\, W$for the $10\, mm/s$ scan speed and $32.5\ J/mm^3$ energy densities for the first coupon and $850\, W$for the $6\ mm/s$ scan speed and $70.8\ J/mm^3$ energy densities for the second coupon. Layer thickness is set to $2.24\ mm$ for the first coupon and $3.03\ mm$ for the second coupon for the deposition. The deposition data set consists of

120 layers and 91000 frames for the first part and 66 layers and 86000 frames for the second part.

A computerised tomography (CT) scan has been done on both parts to identify defects without destruction on the parts. The scan result provides the number of defects per layer for both parts. In this study, a relationship between the number of the defects and outliers identified by the proposed algorithm is assumed.

B. Online outlier detection using a self-tuning multi-model approach

The training of the proposed method starts with the selection of the training data set from the deposition. In this study, the first 11 layers of the part are selected as initial training data set. Fig. 3(b) illustrates the comparison of all layers and the initial training data set. The update in the training dataset follows a moving window principle where the newly deposited layer is added, but the very last layer is removed from the training window.

In Fig. 4, k-means clustering labels for the first training data set is illustrated. Here, the number of the clusters assigned as 4 based on Silhouette scores. This assignment remains constant for the coming updates via the self-tuning mechanism, for the sake of simplicity for this study. A clear separation of the direction and position of the samples in the deposited part can be seen. Even though different separations are observed in the first 3 layers, similar patterns are acquired in the following layer. This is because of the difference between the interaction of the melting points with ground zero and the deposited part. The aforementioned path planning for the first coupon that is related to the same starting point for each layer can also be seen around origin of the x-axis where these behaviours clustered under cluster-4.

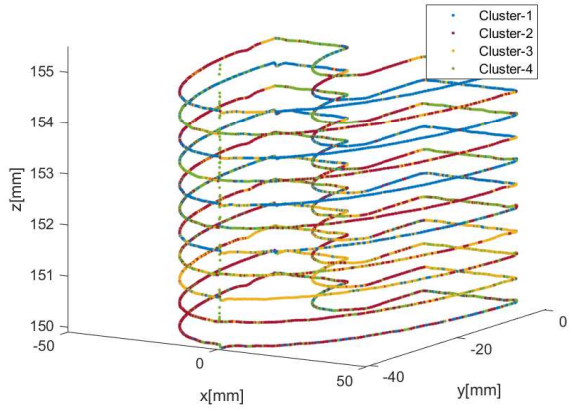

Fig. 4. Illustration of the cluster separation on the training data set acquired from the first coupon.

Following the initial clustering in Fig. 4, MPCA models are trained from the meltpool images assigned into the related clusters to reduce the size of the dimensions while keeping the explained variances high. One of the parameters for the MPCA modelling to identify the number of the reduced size of features is the level of the explained variance. 90% level of explained variance is selected for each MPCA model. Due to the complex process dynamics of the AM, the meltpool characteristics tend to change through the deposition due to the nature of the path planning and the design of the print parameters.

In this study, the training data set and MPCA models change with every layer by following the moving window principle that always provides 11 layers long training data set for clustering and consequently MPCA modelling. After successful modelling, the T^2 metric evaluation for the next layer is done for the detection of the outliers; once the next layer is printed, the training-forecasting process is repeated. It is worth noting that the outliers identified in this stage are not involved in the training data set for the next iteration of the self-tuning scheme due to suspected abnormalities of the samples.

Initial MPCA models for each sample cluster provided around 80% total reduction in the size of the original thermal image where they convert 64×64 tensor to $12 \times 12, 12 \times 15, 10 \times 10, 11 \times 11$ matrices for 90% level of explained variance, respectively. Even though these numbers are for the first training data set the remaining iterations for the self-tuning followed the same trend. Determination of the control limits for the T^2 is another important point for the outlier detection where it can be determined as $(1-\alpha)100^{th}$ percentiles of the F-distribution. However, these normality assumptions for features and residual distributions are not valid in some cases. In such cases like this study, the empirical distributions are estimated using the training samples which are in control. In this study, 3 different control limits are tested for both parts where they are assigned by using 2.2, 2.5 and 3 times of the standard deviation of the empirical distributions of the training data set.

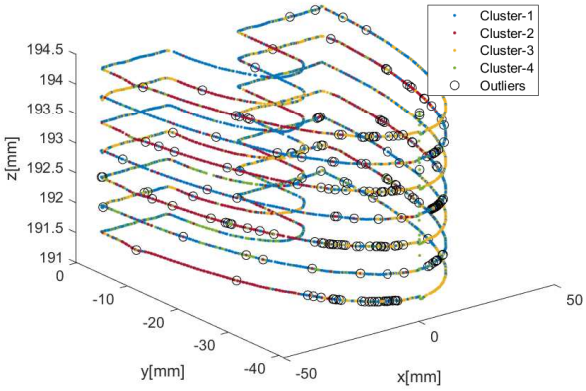

Fig. 5. Illustration of the testing data set with the outlier identified by the MPCA models based on 2.2σ for the first coupon.

Fig. 5 illustrates the outliers on the testing data sets for the first coupon based on 2.2 times the standard deviation. Here,

detected outliers are dense on the outer c-shape where the angle of the wall is suitable for the defects considering the single bead based deposition. Defects frequency also follow the beam path of the deposition where we see more outliers in the direction of the path around the starting point for the first part. The frequent outlier side alternates in every layer from the starting point.

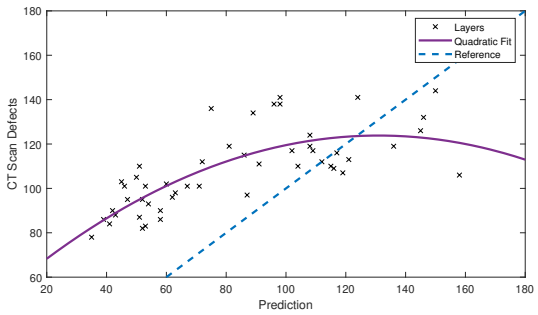

Fig. 6. Illustration of the quadratic fit on the number of defects versus the predicted number of the outlier where the reference represents one to one matching.

Fig. 6 illustrates the number of defects found from the CT scan and the number of outliers from the proposed methodology. The samples represent 50 layers after the initial 11 layers for the base training. There is a clear relationship between the number of outliers detected and defects measured. It is possible to fit a function (linear, quadratic etc.) that would account for the mapping between outliers and defects. In our case, a quadratic function is estimated to project this bias: $b = -004511a^2 + 1.181a + 46.48$. Table I tabulates mean absolute percentage errors (MAPEs) of the remained testing layers that are not used in the calibration according to

$$MAPE = \frac{100}{M} \sum_{m=1}^{M} \left| \frac{A_m - F_m}{A_m} \right| \tag{10}$$

where A_m and F_m are the number of defects from the CT scan and the proposed algorithm after the calibration. M is the number of the remained sample of layers. Here, each calibration is done separately for each control limit and coupon combination. Choosing 2.2σ for the first coupon results in good prediction response in comparison with the other control limits. On the other hand, the second coupon shows different characteristics in the calibration phase where the higher control limits results in better defect forecasting. Note that higher control limits can result in fewer outliers above the limits if the T^2 metric is assumed as well-distributed.

TABLE I
MAPE [%] VALUES FOR THE DIFFERENT CONTROL LIMITS.

Coupon No—Control Limit	2.2σ	2.5σ	3σ
1	**10.80**	11.13	11.66
2	22.75	21.49	**15.89**

IV. Conclusion

In this study, we presented an in-situ monitoring method for AM based on image streams. To the best of our knowledge, it is the first deployment of a multi-model approach based on SPC and MPCA where extracted image features are clustered together to define the multi-model characteristics. In-situ implementation is achieved via a self-tuning mechanism that uses a sliding window approach to add/drop layers to the training dataset iteratively. This results to multi-model framework, that continuously adapts to part design.

The proposed outlier detection scheme is tested on two LMD parts, of the same design, but manufactured under different process conditions. Results demonstrate there is a correlation between the outliers predicted and the measured part defects. This relationship can be modelled, in each case, using simple functions as a way to calibrate the system for the proposed empirical control limits. The best case scenario calibration and control limits, for the two parts, yield above 84% accuracy in forecasting defects.

Acknowledgment

The authors would like to thank Brunel University London, UK, and University of Patras (Laboratory for Manufacturing Systems and Automation: LMS), Greece, for their expert knowledge, information, and data, that supported the work in this manuscript.

References

[1] D. L. Bourell, "Perspectives on Additive Manufacturing," Annu. Rev. of Mater. Res., vol. 46, no. 1, pp. 1–18, Jul. 2016, doi: 10.1146/annurev-matsci-070115-031606.

[2] S. K. Everton, M. Hirsch, P. Stravroulakis, R. K. Leach, and A. T. Clare, "Review of in-situ process monitoring and in-situ metrology for metal additive manufacturing," Mater. Des., vol. 95, pp. 431–445, Apr. 2016, doi: 10.1016/j.matdes.2016.01.099.

[3] M. Mani, B. M. Lane, M. A. Donmez, S. C. Feng, and S. P. Moylan, "A review on measurement science needs for real-time control of additive manufacturing metal powder bed fusion processes," Int. J. of Production Res., vol. 55, no. 5, pp. 1400–1418, Aug. 2016, doi: 10.1080/00207543.2016.1223378.

[4] S. Barua, F. Liou and J. Newkirk, "Vision-based defect detection in laser metal deposition process," Rapid Prototyping J., vol. 20, no. 1, pp. 77–85, 2014,

[5] B. M. Colosimo and M. Grasso, "Spatially weighted PCA for monitoring video image data with application to additive manufacturing," J. of Qual. Technol., vol. 50, no. 4, pp. 391–417, Oct. 2018, doi: 10.1080/00224065.2018.1507563.

[6] M. Grasso, V. Laguzza, Q. Semeraro and M. Colosimo "In-process monitoring of slective laser melting: spatial detection of defects via image data analysis," J. of Manuf. Sci. and Eng., vol. 139, no. 5, May 2017, doi: 10.1115/1.4034715.

[7] H. Yan, K. Paynabar, and J. Shi, "Image-Based Process Monitoring Using Low-Rank Tensor Decomposition," IEEE Trans. on Autom. Sci. Eng., vol. 12, no. 1, pp. 216–227, Jan. 2015, doi: 10.1109/tase.2014.2327029.

[8] M. Khanzadeh, W. Tian, A. Yadollahi, H. R. Doude, M. A. Tschopp, and L. Bian, "Dual process monitoring of metal-based additive manufacturing using tensor decomposition of thermal image streams," Additive Manuf., vol. 23, pp. 443–456, Oct. 2018, doi: 10.1016/j.addma.2018.08.014.

[9] H. Lu, K. N. Plataniotis, and A. N. Venetsanopoulos, "MPCA: Multilinear Principal Component Analysis of Tensor Objects," IEEE Trans. on Neural Netw., vol. 19, no. 1, pp. 18–39, Jan. 2008, doi: 10.1109/TNN.2007.901277.